BL-8B/2023G513

High T_c superconductivity of high-pressure phase stabilized quasi-stably in severely strained barium

Masaki MITO[1,*] and Takayuki TAJIRI[2]
[1] Kyushu Institute of Technology, Kitakyushu 804-8550, Japan
[2] Fukuoka University, Fukuoka 814-0180, Japan

In the alkali-earth metal barium, superconductivity appears after structural transformation from body-centered cubic structure to hexagonal-close-packed (hcp) structure at hydrostatic pressure (P_{HP}) of 5 GPa, and the superconducting transition temperature (T_c) reaches a maximum of 5 K at P_{HP} = 18 GPa. Furthermore, by structurally stabilizing the low temperature phase at P_{HP} ~ 30 GPa, T_c reached a higher level of 8 K. We demonstrated a significantly higher T_c superconductivity in Ba at ambient pressure, which experienced severe plastic deformation by high-pressure torsion (HPT). In this HPT-processed Ba, we observed superconductivity at T_c = 3 K and T_c = 24 K in the quasi-stabilized hcp and orthorhombic structures, respectively. The study demonstrates the importance of utilizing high-pressure strained phases as the creation of superconducting states at ambient pressure.

1 Introduction

Among the 118 elements in the periodic table, about one-fourth is ambient-pressure superconductor, and one-fifth becomes superconductors under hydrostatic pressure [1]. These are classified as *s*, *s*-*d*, *s*-*p*, and *s*-*f* electron systems, respectively. In alkali and alkali-earth metals, *s*-electrons significantly influence electric properties. Heavier alkali and alkali-earth metals, such as Cs, Ca, Sr, and Ba, exhibit transition into *s*-*d* electron superconductors accompanying pressure-induced structural transformation from body-centered cubic (bcc) to other crystal structures, where electron transfer from *s*- to *d*-orbitals plays a crucial role [2]. Many researches, especially on Ba, focuse on hydrostatic contraction effects [3-8]. Thus, reduction in structural symmetry and structural phase transformation are crucial for stabilizing superconducting state in these metals. Therefore, manipulating lattice strain and crystal structures could be effective to enhance T_c. In this study, we utilized a high-pressure torsion (HPT) process to introduce shear and compressive strains.

In HPT, the magnitude of shear strain increases in proportion to the distance from the disk center, as well as the number of revolutions *N*. Herein, the compressive stress allows only the diagonal components in the strain tensor, whereas the shear strain leads to the nondiagonal components. In Ba, the presence of a variety of high-pressure phases under hydrostatic pressure (P_{HP}) [4] has been reported so far: In particular, a high-pressure phase Ba-VI (orthorhombic) stabilized at P_{HP} = 12–30 GPa and temperatures below 150 K appears to be the most suitable candidate for high T_c [3, 4].

In this study, we utilize the HPT process to stabilize such high-pressure hcp and orthorhombic phases even under ambient pressure. Our findings demonstrate that these resulting high-pressure phases can maintain their stability even after the stress is released [9].

2 Experiment

Processing through high-pressure torsion (HPT) causes severe plastic deformation [10, 11]. First, a disk sample was uniaxially compressed between opposite-faced anvils, which were made of WC (SR16C, NOTOALLOY Co., Ltd.), using a 50-ton press machine. The lower-side anvil was then rotated for *N* revolutions. During the revolution process, severe shear strain accumulates. In the early stage, the grain size was reduced, and subsequent recrystallization proceeded, resulting in a balance between these effects.

In this study, HPT was first conducted at room temperature for *N* = 10 turns under a pressure of P_{HPT} = 6 GPa with a rotation speed of 1 rpm. In this room-temperature HPT process, Ba was easily oxidized and sealed in an Al-Mg-Sc alloy cell under an Ar atmosphere. A Ba disk (purity 99.9%, 7-mm-diameter, 0.6-mm-thickness) in the Al-alloy cell was then processed using an HPT machine. The HPT process was also conducted using disks with dimensions of 5 mm in diameter and 1 mm in thickness so that it was possible to control the applied pressure up to a maximum of P_{HPT} = 24 GPa. The HPT process was performed in liquid nitrogen, where liquid and gaseous nitrogen played a role in preventing the oxidation of the Ba disks instead of the Al-alloy cell.

After HPT, the samples were removed from the HPT apparatus and maintained at 77 K in a liquid nitrogen vessel. The samples were removed from the vessel immediately before the magnetic measurements and X-ray diffraction (XRD) experiments. For the magnetic measurements, the samples were placed under ambient pressure conditions, and the temperature was cooled to 1.8 K. XRD experiments were conducted under ambient pressure and room temperature for samples coated with paraffin oil to prevent oxidization.

First, we have formed reflection-type XRD at room temperature using SmartLab (Rigaku) para-focusing optics with Cu ($K\alpha_1$ and $K\alpha_2$) radiation. We also used thrubeam-type XRD analysis using synchrotron radiation with an X-ray energy of 16 keV at the beamline BL-8B in KEK-PF. The observed diffraction peaks were deconvolved using the Voight function into those associated with each Ba phase by multipeak fitting. The lattice constants were calculated from the relationship between the lattice constants and the plane indices determined from the Bragg peak angles of the deconvoluted peaks. All the crystal structures were

evaluated based on the assumption that the atomic positions did not change.

3 Results and Discussion

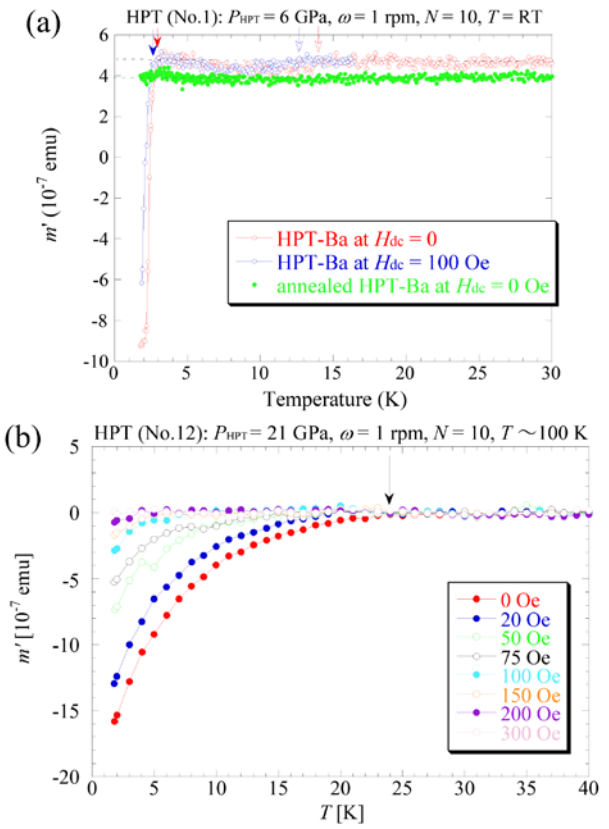

Fig. 1: (a) Temperature dependence of in-phase AC magnetization m' for Ba (sample No.1) subjected to HPT at room temperature, where P_{HPT} and N were 6 GPa and 10, respectively. During HPT, a Ba disk was encapsulated in an Al-based cell to prevent oxidization. The results after annealing the HPT-processed Ba at 503 K in a vacuum for one hour is also shown. During the HPT processing at P_{HPT} = 6 GPa and room temperature (RT), the targeted high-pressure phase was the hcp phase. (b) Temperature dependence of m' for Ba (sample No.12) subjected to HPT at liquid-nitrogen temperature, where the P_{HPT} value was 21 GPa and the N value was 10. The targeted high-pressure phase is the orthorhombic phase.

Figure 1(a) shows the temperature (T) dependence of the in-phase AC magnetization m' for HPT-processed Ba (P_{HPT} = 6 GPa, N = 10 at room temperature). A diamagnetic signal was unambiguously observed at 3 K in HPT-processed Ba. In addition, a small but visible diamagnetic signal was also observed at 14 K. We confirmed that neither signal originated from the Al–Mg–Sc cells subjected to HPT processing. The diamagnetic signals shift to the low-temperature side when a DC magnetic field (H_{dc}) of 100 Oe is applied. There we also show results obtained after annealing the HPT-processed Ba at 503 K in a vacuum for one hour. No diamagnetic signals are observed in the sample after annealing. The annealing temperature of 503 K is more than half the melting point of Ba (999 K) and is enough to release the residual strain.

The superconducting properties of HPT-Ba were also investigated at cryogenic temperatures, where HPT processing was performed at P_{HPT} = 12–24 GPa for N = 10, and the processing temperature was maintained at approximately 100 K in liquid nitrogen. Figure 1(b) shows the T dependence of m' for the HPT-processed sample at P_{HPT} = 21 GPa, where the magnetic shielding signal appears at approximately 24 K under H_{dc} = 0 Oe and disappears at H_{dc} = 300 Oe. We emphasize that this T_c is the highest achieved at ambient pressure for pure metals, although higher values of T_c than 24 K have been reported under the application of high pressures such as scandium (36 K at 260 GPa) [12], titanium (26 K at 240 GPa) [13, 14], and calcium (29 K at 220 GPa) [15].

Structural analysis results of an HPT-processed Ba specimen (sample No. 8) for P_{HPT} = 6 GPa and N = 10 at room temperature are summarized in Table 1. It is demonstrated that the high-pressure phase, hcp phase, with the volume fraction of approximately 7 % is included along with three bcc phases. Thus, we have succeeded in stabilizing the high-pressure phase exhibiting superconductivity by the HPT processing even after the stress is released.

Acknowledgement

We thank Prof. Z. Horita (Kyushu Institute of Technology) for the collaboration in the HPT processing. This work was also supported by Grant-in-Aid for Scientific Research, Grant No. 23H01126, from MEXT, Japan.

References

[1] J. J. Hamlin, Superconductivity in the metallic elements at high pressures, *Physica C* (Amsterdam, Neth.) **514**, 59–76 (2015).
[2] J. S. Schilling, High-Pressure Effects, in Handbook of High-Temperature Superconductivity, edited by J. R. Schrieffer, pp.427–462 (Springer, New York, 2007)
[3] K. Shimizu *et al.*, Pressure-induced superconductivity in elemental materials. *J. Phys. Soc. Jpn.* **74**, 1345–1357 (2005).
[4] S. Desgreniers *et al.*, High pressure–low temperature phase diagram of barium: Simplicity versus complexity. *Appl. Phys. Lett.* **107**, 221908 (2015).
[5] D. E.Jackson *et al.*, Superconductivity of barium-VI synthesized via compression at low temperatures. *Phys. Rev. B* **96**, 184514 (2017).
[6] J. Wittig and B. T. Matthias, Superconductivity of barium under pressure. *Phys. Rev. Lett.* **22**, 634 (1969).
[7] A. R. Moodenbaugh and J. Wittig, Superconductivity in the high-pressure phases of barium. *J. Low Temp. Phys.* **10**, 203 (1973).
[8] C. Probst and J. Wittig, Superconductivity of bcc barium under pressure. *Phys. Rev. Lett.* **39**, 1161 (1977).
[9] M. Mito, T. Tajiri *et al.*, Superconductivity of barium with highest transition temperatures in metallic materials at ambient pressure, *Sci. Rep.* **14**, 965 (2024) .
[10] A. P. Zhilyaev and T. G. Langdon, Using high-pressure torsion for metal processing: Fundamentals and applications. *Prog. Mater. Sci.* **53**, 893–979 (2008).
[11] K. Edalati and Z. Horita, Z. A review on high-pressure torsion (HPT) from 1935 to 1988. *Mater. Sci. Eng. A* **652**, 325–352 (2016).
[12] J. Ying, *et al.*, Record high 36 K transition temperature to

the superconducting state of elemental scandium at a pressure of 260 GPa. *Phys. Rev. Lett.* **130**, 256002 (2023).
[13] X. Liu, *et al*., *T*c up to 23.6 K and robust superconductivity in the transition metal δ-Ti phase at megabar pressure. *Phys. Rev. B* **105** , 224511 (2022).
[14] C. Zhang, *et al*. Record high *T*c element superconductivity achieved in titanium. *Nature Commun.* **13**, 5411 (2022).
[15] M. Sakata, *et al*., Superconducting state of Ca-VII below a critical temperature of 29 K at a pressure of 216 GPa. *Phys. Rev. B* **83**, 220512(R) (2011).

* mitoh@mns.kyutech.ac.jp

Table 1: Structural analysis results of thrubeam XRD experiments for HPT-Ba (No. 8) at P_{HPT} = 21 GPa.

P_{HPT}	phase	a [Å]	b [Å]	c [Å]	c/a	V_{atom} [Å^3]	V_{atom}/V_0	P_{HP} [GPa]	wt%
No.8: 6 GPa, N = 10, RT									
(much oxidized)	bcc #1	5.136 ± 0.007	5.136 ± 0.007	5.136 ± 0.007	-	67.740	1.069	-0.8	78.3
(PF, KEK)	bcc #2	4.919 ± 0.008	4.919 ± 0.008	4.919 ± 0.008	-	59.511	0.939	0.8	9.3
	bcc #3	4.670 ± 0.034	4.670 ± 0.034	4.670 ± 0.034	-	50.924	0.804	2.5	5.8
	total bcc	-	-	-	-	-	-	-	93.4
	hcp #1	3.824 ± 0.025	3.824 ± 0.025	6.022 ± 0.049	1.574	38.131	0.601	7.0	6.6
	total hcp	-	-	-	-	-	-	-	6.6